

INSTITUTE FOR FUSION STUDIES

DE-FG05-80ET-53088-693

IFSR #693

Quantitative Predictions of Tokamak Energy Confinement from First-Principles Simulations with Kinetic Effects

M. KOTSCHENREUTHER, W. DORLAND

Institute for Fusion Studies

The University of Texas at Austin

Austin, Texas 78712

and

M.A. BEER, G.W. HAMMETT

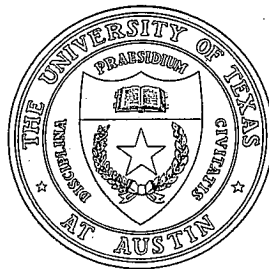
Princeton Plasma Physics Laboratory

P.O. Box 451

Princeton, NJ 08543

March 1995

THE UNIVERSITY OF TEXAS



AUSTIN

Quantitative Predictions of Tokamak Energy Confinement from First-Principles Simulations with Kinetic Effects

M. Kotschenreuther, W. Dorland

Institute for Fusion Studies, The University of Texas at Austin

Austin, Texas 78712

and

M. A. Beer, G. W. Hammett

Princeton Plasma Physics Laboratory, P. O. Box 451, Princeton, NJ, 08543

Abstract

A first-principles model of anomalous thermal transport based on numerical simulations is presented, with stringent comparisons to experimental data from the Tokamak Fusion Test Reactor (TFTR) [Fusion Technol. **21**, 1324 (1992)]. This model is based on nonlinear gyrofluid simulations, which predict the fluctuation and thermal transport characteristics of toroidal ion-temperature-gradient-driven (ITG) turbulence, and on comprehensive linear gyrokinetic ballooning calculations, which provide very accurate growth rates, critical temperature gradients, and a quasilinear estimate of χ_e/χ_i . The model is derived solely from the simulation results. More than 70 TFTR low confinement (L-mode) discharges have been simulated with quantitative success. Typically, the ion and electron temperature profiles are predicted within the error bars, and the global energy confinement time within $\pm 10\%$. The measured temperatures at $r/a \simeq 0.8$ are used as a boundary condition to predict the temperature profiles in the main confinement zone. The dramatic transition to the improved confinement in the supershot regime is also qualitatively explained. Further work is needed to extend this model of core heat transport

to include particle and momentum transport, the edge region, and other operating regimes besides the ITG-dominated L-mode. Nevertheless, the present model is very successful in predicting thermal transport in the main plasma over a wide range of parameters.

I. INTRODUCTION

A firm scientific understanding of anomalous transport in magnetically confined plasmas has remained elusive despite decades of effort. The need for a sound, first principles, quantitative understanding is particularly acute now. Reliable methods are needed to project the performance of proposed designs for the next generation of large fusion experiments aimed at ignition. Ideally, such predictive methods would not neglect important physical effects in the name of tractability, would not employ ad-hoc or unjustifiable assumptions, and would not be primarily empirical fits to data without a sound theoretical understanding of the associated range of validity. Of course, such methods would also accurately predict the performance of the present generation of experiments. We report here significant progress in developing a method that meets all of these criteria.

For several years, it has been widely appreciated that plasma turbulence is probably too complex to describe quantitatively without employing large-scale computer simulations. By 1990, two important breakthroughs – the δf particle simulation algorithm^{1,2} and a new class of fluid models of wave-particle interactions^{3,4} – had already led to dramatically faster and more realistic turbulence simulations,^{1,5} albeit in sheared-slab geometry. Because the turbulent transport from these sheared-slab simulations was too small to explain the experimental data,¹ toroidal generalizations⁶⁻⁸ were developed and implemented.⁹ Here, we report that a predictive method based on such simulations has been developed and tested on a large number of Tokamak Fusion Test Reactor¹⁰ (TFTR) low confinement (L-mode) discharges. Quantitative predictions of core energy confinement times and temperature profiles have been obtained.¹¹ Furthermore, the method produces good qualitative agreement with core confinement behavior in other tokamak operating modes, such as supershots and hot-ion modes, high inductance ℓ_i modes, high confinement (H-mode) discharges, and others.

Two important advances account for the success of the present model. One is the de-

velopment of fairly realistic, nonlinear, gyrofluid simulations of toroidal ion-temperature-gradient-driven (ITG) turbulence, which are described briefly in Sec. II and in more detail in Refs. 12 and 13. Toroidal effects (especially bad-curvature drive and neoclassical damping of nonlinearly generated sheared flows) are crucial. The other important advance is the development of a successful interpolation formula to parameterize the resulting χ_i , including an accurate calculation of the critical temperature gradient by a comprehensive linear gyrokinetic ballooning code. Because most plasmas are found to be near marginal stability over some fraction of the minor radius,¹⁴ precise knowledge of the critical temperature gradient is necessary.

II. METHOD

To validate any theory of thermal transport with reasonable confidence, it is necessary to compare the theory with a large number of experimental discharges, and to compare at multiple radial points in each shot. With present resources, it is too costly to perform well-resolved nonlinear simulations for 60 shots at 20 radial comparison points. However, simulations of a flux-tube sub-domain of the torus indicate that χ is a function of local plasma parameters, if the normalized gyroradius $\rho_* = \rho_i/L_{n,T}$ is small enough.^{13,15} Thus, we develop an interpolation formula for χ as a function of local plasma parameters from nonlinear gyrofluid simulations. These simulations are supplemented with linear gyrokinetic simulations using a code with comprehensive fully kinetic physics.¹⁴ We emphasize that the resulting formula is a fit to first principles simulations. *No reference to experimental data was made to construct the formula.* The χ formula is simply the best reasonably simple approximation we have been able to devise to the best first principles simulation results available.

The 6-moment toroidal gyrofluid equations and the nonlinear gyrofluid code utilized

here are described in detail in Ref. 12. These equations describe “kinetic” effects such as toroidal drift resonances,^{7,12} linear and nonlinear FLR orbit-averaging,¹⁶ and parallel wave-particle resonances^{3,4} for an arbitrary number of ion species, and are evolved in toroidal field-line-following (FLF) coordinates.^{13,17} Nonlinear gyrofluid trapped electron models^{12,15} and generalized FLF coordinates¹³ have recently been developed, but are not employed here. One of the important features of these simulations is the self-consistent treatment (including transit-time magnetic pumping¹²) of nonlinearly generated,¹⁸ fine scale ($k_r \rho_i \sim 0.1$), sheared poloidal flows, which play a major role in determining the saturation level for the turbulence.

The nonlinear simulations completed for this study typically had 2000–4000 independent modes (k_r, k_θ) on a 32–64 point FLF grid. The simulated volume was typically $63\rho_i \times 63\rho_i \times 2\pi qR$ (*i.e.*, $\sim 1.5\%$ of the total TFTR plasma volume), and the total simulated time was typically 50–100 growth times, or $250 L_n/v_t \simeq 0.5 \text{ msec}$ for typical tokamak conditions. Larger-scale and longer-time simulations have been completed to demonstrate convergence.^{13,17}

The comprehensive gyrokinetic code^{14,19} has full velocity space dynamics including resonances, trapped particles, Coulomb collisional pitch angle diffusion, *etc.* The gyrofluid simulations obtain the nonlinear χ , but have a somewhat inaccurate critical temperature gradient, and also neglect non-adiabatic electron physics. The comprehensive linear code corrects the formula for this.

The construction of an interpolation formula still encounters difficulties because of the large number of parameters in the governing equations. The gyrokinetic equation depends on R/L_T , R/L_n , q , \hat{s} , T_i/T_e , Z_{eff} , ν , r/R , *etc.* To map out parameter space thoroughly requires an unacceptable number of nonlinear runs. However, we have found a novel method that greatly reduces the number of nonlinear runs required. We have observed from the nonlinear simulations that the ratio $W_{\text{NL}} \equiv \chi/D$ is a much weaker function of parameters

than χ itself. Here, $D \equiv \max(\gamma/k_{\perp}^2)$, where

$$k_{\perp}^2 = \frac{\int d\theta |\Phi|^2 (\nabla S)^2}{\int d\theta |\Phi|^2} \approx k_{\theta}^2 (1 + \hat{s}^2 \langle \theta^2 \rangle)$$

and we take the maximum value of γ/k_{\perp}^2 over all k_{θ} . We use the gyrofluid code to calculate W_{NL} based upon the nonlinearly obtained χ and the gyrofluid D^{GF} . We then calculate D^{GK} with the comprehensive linear gyrokinetic code. The formula for χ_i that appears below is an interpolation of $W_{NL} D^{GK}$.

Of course, fewer points are needed to interpolate W_{NL} since it is a weakly varying function. The reduction in the number of nonlinear runs needed can be enormous. If we parameterize W_{NL} over the nine dimensions R/L_T , R/L_n , q , \hat{s} , T_i/T_e , r/R , ν , n_b/n_e , and Z_{eff} , and reduce the number of points needed in each dimension by only a factor of 2, then the total number of nonlinear runs needed is reduced by a factor of $2^9 = 512$. Many hundreds of much less expensive linear runs were used to map out D^{GK} .

III. INTERPOLATION FORMULAE

The simulations are best characterized by a strong deuterium toroidal ITG mode with critical gradient scale length $R/L_{T\text{crit}}^{(1)}$, and a weak carbon toroidal ITG mode with critical gradient scale length $R/L_{T\text{crit}}^{(2)}$. The carbon mode is observed when the thermal charge fraction of carbon $\sigma_C \equiv 6(n_C/n_e)/(1 - \sigma_b) \sim 0.5$ or greater, where σ_b is the energetic particle (beam) charge fraction.¹¹ That $R/L_{T\text{crit}}^{(2)} < R/L_{T\text{crit}}^{(1)}$ is known.²⁰ The carbon mode is important in the supershot regime, but irrelevant in the L-mode regime. Our interpolation of the simulation results is:

$$\chi_i = C_0 \max(\chi_i^{(1)}, \chi_i^{(2)}) \rho_i^2 v_{ti}/R, \quad (1)$$

in which $C_0 = 12$,

$$\chi_i^{(1)} = \frac{(q/\tau_b)^{1.1}}{1 + \hat{s}^{0.84}} \left(1 + \frac{6.7\epsilon}{q\nu^{0.26}} \right) \mathcal{Z}(Z_{\text{eff}}^*) \mathcal{G}^{(1)}(R/L_T)$$

and

$$\chi_i^{(2)} = \frac{0.33\tau_b^{-0.8}}{1 + \hat{s}} \max[0.5, (Z_{\text{eff}}^* - 3)] \mathcal{G}^{(2)}(R/L_T).$$

Here, $\mathcal{G}^{(i)} \equiv G(R/L_T - R/L_{T_{\text{crit}}^{(i)}})$, $G(x) \equiv \min(x, x^{1/2})H(x)$, and $H(x)$ is a Heaviside function. The temperature ratio $\tau \equiv T_i/T_e$, $\tau_b \equiv \tau/(1 - \sigma_b)$, and $\mathcal{Z} = \min[1, (3/Z_{\text{eff}}^*)^{1.8}]$. The expression $Z_{\text{eff}}^* \equiv (n_D + 36n_C)/(n_D + 6n_C)$, where n_D is the thermal hydrogenic ion density, and only carbon impurities n_C have been considered. [High Z impurities tend to cause little dilution and can usually be ignored, while low-Z impurities such as helium are not well described by this parameterization.] The collisionality parameter $\nu \equiv 2.1 R n_{e19}/(T_e^{1.5} T_i^{0.5})$, where R is given in meters and the temperatures are in keV. All other symbols are standard.²¹

The critical gradient scale length of the deuterium mode is approximately

$$R/L_{T_{\text{crit}}}^{(1)} = f(\{p_j\}) g(\{p_j\}) h(\{p_j\}), \quad (2)$$

where $f = 1 - 0.2Z_{\text{eff}}^{*0.5}\hat{s}^{-0.7}(14\epsilon^{1.3}\nu^{-0.2} - 1)$, $g = (0.7 + 0.6\hat{s} - 0.2R/L_n^*)^2 + 0.4 + 0.3R/L_n^* - 0.8\hat{s} + 0.2\hat{s}^2$, and $h = 1.5(1 + 2.8/q^2)^{0.26} Z_{\text{eff}}^{*0.7}\tau_b^{0.5}$. Here, $R/L_n^* \equiv \max(6, R/L_n)$ and all density scale lengths are assumed to be equal. The critical gradient scale length of the carbon mode is approximately

$$R/L_{T_{\text{crit}}}^{(2)} = 0.75(1 + \tau_b)(1 + \hat{s})\mathcal{D}(R/L_n^*)\mathcal{E}(Z_{\text{eff}}^*) \quad (3)$$

in which $\mathcal{D} \equiv \max(1, 3 - 0.67R/L_n^*)$ and $\mathcal{E} \equiv 1 + 6 \max(0, 2.9 - Z_{\text{eff}}^*)$.

The electron χ_e is obtained from the ratio of the quasilinear electron and ion heat fluxes found with the comprehensive linear code. For the deuterium mode, $\chi_e^{(1)}/\chi_i^{(1)} = 0.72\epsilon^*\nu^{0.14}(q/\hat{s})^{0.3}\tau^{0.4}\mathcal{J}_{1.5}(R/L_n)$. Here, $\epsilon^* \equiv \max(0.17, \epsilon)$. For the carbon mode, $\chi_e^{(2)}/\chi_i^{(2)} = 0.26\tau\nu^{0.22}\mathcal{J}_2(R/L_n^*)$. In these expressions, $\mathcal{J}_\xi \equiv \max[\xi, (1 + 0.3R/L_n^*)]$. Finally,

$$\chi_e = C_0 \max(\chi_e^{(1)}, \chi_e^{(2)}) \rho_i^2 v_{ti}/R. \quad (4)$$

Both passing and trapped non-adiabatic electron effects contribute significantly to these formulae. The qualitative trends we observe conform to those previously known in the

literature.^{22,23} Stabilizing trends result from increasing T_i/T_e , deuterium dilution by carbon or beams, and magnetic shear \hat{s} . Increasing q is destabilizing, as are trapped particle effects, which are moderated by collisions.

The unique feature of these formulae is that they were obtained from state of the art simulations that include relevant physics as well as presently possible. Thus, they are the most quantitatively credible theoretical formulae for χ from ITG turbulence presently available. Furthermore, they are a fairly simple distillation of the most salient results from a great deal of computational expense and human effort in code development. Nevertheless, the formulae have limitations. The interpolation formulae are only derived for normal tokamak parameters: $0.7 < q < 8$, $0.5 < \hat{s} < 2$, $0 < R/L_n < 6$, $0.5 < T_i/T_e < 4$, $1 < Z_{\text{eff}} < 4$, $0.5 < \nu < 10$, $0.1 < r/R < 0.3$, *etc.* Thus, they should not be expected to reproduce extreme limits, such as ν approaching zero or infinity, shear approaching zero, *etc.* Furthermore, for low collisionality and strong density gradients, a trapped electron drift wave instability appears that is not treated in these formulae. The carbon branch formulae are more approximate than the formulae for the deuterium branch. Finally, physical effects such as velocity shear, gradients of Z_{eff} , and non-circular flux surfaces are important for some experiments, but are not included above.

IV. EXPERIMENTAL COMPARISONS

The limitations in Eqs. (1)–(4) are expected to be unimportant for typical circular L-mode plasmas in the region $0.25 < r/a < 0.8$. We now turn to experimental comparisons with TFTR data for such plasmas.

Before using results from simulations with kinetic effects to design future experiments, it is necessary to demonstrate a predictive capability on present experiments. Unlike other models,²⁴ our theory does not yet attempt to predict particle transport or convection. In-

stead, we use HYPED,²⁵ which is a 1-d steady state power balance code that runs as a post-processor to either SNAP²⁶ or TRANSP.²⁷ This code has been modified to include Eqs. (1-4), and otherwise includes the standard TFTR power balance assumptions: classical electron-ion temperature equilibration, beam slowing down, neoclassical Ohmic heating and neoclassical χ_i , *etc.* The code accepts the experimentally measured density profile, the inferred q profile and power deposition profile, the measured radiation loss profile, *etc.* The experimentally inferred convective term is used in the power balance calculation (assuming each particle carries $3/2T$ energy). These convective heat losses are small compared to the predicted conduction heat loss except in the core of supershots and near the plasma edge. Under these assumptions, the ion and electron temperature profiles are calculated. We have observed that the χ in Eqs. (1-4) is often smaller than experimentally inferred values in the last 10-20% of the minor radius. Therefore, we have used the experimentally determined temperature as the boundary condition at $r/a \simeq 0.8$.

A. TFTR L-mode Confinement

We have tested the predictive abilities of Eqs. (1-4) on more than seventy L-mode shots and about two dozen supershots. A representative L-mode shot (#41309) is shown in Fig. 1. This discharge (particularly the $r/a = 0.5$ point) was selected in 1992 as the primary comparison case for the Numerical Tokamak Project (NTP). Using HYPED, the temperature profile inside $r/a \simeq 0.8$ has been predicted, along with χ over the same region, with very good agreement (including at $r/a = 0.5$).

Figure 1 demonstrates a number of features common to the other L-mode cases simulated. The temperature predictions are almost always within the error bars or are very close. A universal feature is that the χ increases radially over the confinement zone (typically until $r/a = 0.8 \pm 0.1$). This has been a severe shortcoming of almost all ITG and drift wave

models in the past, which usually predict that χ decreases in the confinement zone due to the gyroBohm factor that is proportional to $T^{3/2}$ in such theories. In the present theory, χ increases with minor radius primarily because the deviation from marginality is increasing.¹⁴

Although the plasma is close to the marginal stability threshold at the center, it is well above threshold towards the edge, as shown in Fig. 2. Thus, a model based upon a strong marginal stability hypothesis for $r/a < 0.8$ would not predict the experimental temperatures accurately. Typically, the central temperatures predicted under this assumption are too low by a factor of ~ 2 . This demonstrates the importance of the nonlinear simulations to this study.

A summary of the results of 63 L-mode cases is shown in Fig. 3, in which the predicted energy confinement times and the measured values are compared. Also shown in Fig. 3 are results from two empirical models that are presently used to design the next generation of experiments: the International Thermonuclear Experimental Reactor confinement scaling²⁸ (ITER89-P) and the Rebut-Lallia-Watkins (RLW) model [To calculate the temperature profiles and energy confinement times predicted by the RLW model, we used the experimental temperature at $r/a = 0.8$ as the boundary condition.] For all cases, the same definition of τ_E is used as in ITER89-P.²⁸ The first-principles model is significantly closer to the experimental results.

Confinement in L-modes is empirically found to display nearly universal trends with several dependent variables for a wide variety of tokamaks. These are quantified²⁸ in the ITER89-P empirical scaling law: $\tau_E = 0.048 I_p^{0.85} R^{1.2} a^{0.3} n^{0.1} B^{0.2} (M\kappa/P)^{0.5}$. To test the correctness of Eqs. (1-4) for L-mode core confinement, we have examined numerous parameter scans of TFTR which show these parameter variations. Predicted temperature profiles for a power scan are shown in Fig. 4 (where power varies by a factor of four). The agreement is within or very close to the error bars. As shown in Table I, the predicted τ_E shows the same degradation as ITER89-P, but agrees more closely with experiment. Ion temperature

profiles for an I_P scan are shown in Fig. 5, again with good agreement. The measured τ_E is well-predicted for this scan (Table II). Similar levels of agreement are found in density, aspect ratio, and toroidal magnetic field scans. Also, similar levels of agreement are found for the $T_e(r)$ profiles.

Figure 6 shows the ratio of the predicted $T_i(r)$ to the measured $T_i(r)$ for 70 TFTR L-mode discharges, with widely varying current, power, density, *etc.* As can be seen, the typical error is within $\pm 15\%$. Though a thorough error analysis has not been completed, we believe that the scatter in this figure is consistent with known measurement errors in T_i , and in Z_{eff} , $q(r)$, and $T(r/a = 0.8)$, which affect the theoretical prediction of $T_i(r)$.

While toroidicity-induced ITG turbulence has been a leading candidate to explain tokamak transport, until now it has not been possible to identify it as the main thermal transport mechanism. Now that a reliable theoretical expression for ITG transport has been obtained, Fig. 6 shows that ITG turbulence is in fact the dominant transport mechanism in the core region of TFTR L-modes under widely varying conditions.

Since toroidal ITG transport explains the parameter scaling of ITER89-P on TFTR, it is likely to be responsible for transport in other machines that scale similarly. However, we must warn that Eqs. (1–4) do not include effects that are significant in some other experiments (such as non-circular geometry), so quantitative comparisons of such cases must await their inclusion.

It is important to understand how sensitive the temperature predictions are to possible errors in the theory. We have performed a sensitivity analysis on Eqs. (1–4) for typical L-mode cases to determine this. First, the coefficient C_0 in χ_0 was varied. For typical L-modes, the resulting central temperature predictions varied only as $C_0^{-0.25}$, and the global energy confinement time varied only as $C_0^{-0.15}$. There are two reasons for this. If there were no critical gradient, the central temperature could be estimated by equating two expressions for the energy confinement time: $a^2/\chi \simeq VnT/P_h$. Because of the gyroBohm $T^{1.5}$ scaling of χ ,

this would imply that $T_0 \propto C_0^{-0.4}$. However, if the profile is close to marginally stable, the temperature gradient is insensitive to C_0 : if C_0 is reduced by half, the deviation from the critical gradient must be increased by two to obtain the same power flow. Since the original deviation from criticality was small, the temperature gradient changes little to adjust for the change in C_0 , so the global temperature profile changes little. Thus, when the critical gradient effect is included, the temperature profile is even less sensitive than $C_0^{-0.4}$, and the code typically finds $T_0 \propto C_0^{-0.25}$. Results of varying C_0 by a factor of two for 70 TFTR discharges are shown in Fig. 6. The value of C_0 obtained from the nonlinear simulations is clearly the best predictor of the experimental data, yet the qualitative results are recovered even for these large variations in C_0 .

On the other hand, the profile is very sensitive to the critical gradient. Upon multiplying the critical gradient expression by an arbitrary factor, we find that $T_0 \propto L_{T_{\text{crit}}}^{-1.2}$, and $\tau_E \propto L_{T_{\text{crit}}}^{-0.5}$. [A figure similar to Fig. 6 is obtained if one varies $L_{T_{\text{crit}}}$ by only 20% (while holding C_0 fixed). The $L_{T_{\text{crit}}}$ of Eq. 2 is the best predictor of the experimental data.] These sensitivity results are significant to our ability to make accurate predictions. The coefficient C_0 is determined *nonlinearly*, and is the most expensive and difficult to obtain accurately. Fortunately, predictions are most sensitive to the *linearly* obtained $L_{T_{\text{crit}}}$, which can be calculated with less uncertainty.

Finally, we tested the sensitivity of predicted confinement to the boundary condition at $r/a = 0.8$. The central temperature $T_0 \propto T^{0.6}(r/a = 0.8)$, and $\tau_E \propto T^{0.5}(r/a = 0.8)$. Thus, edge confinement strongly affects global confinement. This correlates with experimental observations that improved edge recycling, which is correlated with good edge confinement, is associated with good core confinement.

B. Enhanced Confinement Regimes

With the results of the sensitivity analysis and Eqs. (1-4), we can predict what type of shots would have better confinement than L-modes. These would be shots with small $L_{T_{\text{crit}}}$ and high boundary temperatures. From Eq. (2), the strongest factors to give small $L_{T_{\text{crit}}}$ are high T_i/T_e , modest deuterium dilution (from either low Z impurities or beams), and high magnetic shear. These results allow us to explain qualitatively several enhanced confinement regimes: supershots and hot ion modes, high internal inductance ℓ_i modes, and the core confinement of H-modes.

Figure 7 shows a pair of TFTR shots with nearly the same power, line average density, current, and toroidal field, yet with radically different central ion temperatures: $T_0 = 4$ keV versus $T_0 = 30$ keV. Of course, ITER89-P predicts that these shots should be virtually identical. The predictions of Eqs. (1-4) are also shown in Fig. 7; most of the tremendous variation in the central ion temperature is explained by the theory. In supershots, the theory shows that the higher edge temperature and deuterium dilution lead to a significantly higher temperature. Higher temperatures lead to a positive feedback amplification through the parameter T_i/T_e : as temperatures increase, the electron-ion equilibration weakens, so for beam-heated shots T_i pulls away from T_e . This increases T_i/T_e , which further raises both temperatures. Note that this process does not run away indefinitely. In the final steady state in supershots, the power balance code predicts that χ_i drops to such low values that the ion power balance is dominated by residual convection (from the beam fueling), resulting in very high central temperatures. This feature, characteristic of supershots, is consistently qualitatively reproduced.

The calculated temperature profile is found to be sensitive to the hollowness of the profile of Z_{eff} , which is not generally well known. [Although we have neglected the explicit dependences on gradients of Z_{eff} in Eqs. (1-4), the dependences on the local Z_{eff}^* have been

parameterized.] Typical supershot Z_{eff} profiles rise roughly parabolically from 2-2.5 in the center to 4-5 at the edge.²⁹ Predicted temperature profiles are shown for two different Z_{eff} profiles: one with Z_{eff} rising parabolically from 2 to 5, and the other with Z_{eff} rising from 2.5 to 4. The sensitivity to $Z_{\text{eff}}(r)$ in the theory arises primarily from the Z_{eff}^* dependences of the critical gradients. The carbon ITG mode (which is the dominant thermal transport mechanism outside of $r/a \simeq 0.4$ in typical supershots) is stabilized as Z_{eff}^* is lowered in the central region. More hollow Z_{eff} profiles have lower central Z_{eff}^* , leading to steeper temperature gradients (characteristic of $R/L_{T\text{crit}}^{(1)}$) in that region.

We must caution, however, that these results are only qualitative. Additional effects that are not significant in L-modes and that are neglected in Eqs. (1-4) are potentially important in supershot plasmas. In particular, trapped electron modes and rotation shear can be significant in supershots for $r/a \leq 0.5$. The former are likely responsible for the residual convective losses not predicted by our theory at present. Linear calculations suggest that rotation shear stabilization is also quantitatively significant in this region. More work needs to be done to explain these complex shots as accurately as the simpler L-modes, but Eqs. (1-4) suffice to explain why the transport processes present in L-modes are qualitatively strongly reduced in supershots.

Confinement enhancements over ITER89-P are also observed in many machines from high internal inductance ℓ_i operation, in which the current is ramped down to produce a peaked current profile. Such profiles have higher magnetic shear and consequently smaller $L_{T\text{crit}}$ for a given current. (On the other hand, the expression for $\chi_i^{(1)}$ shows that the larger safety factor q in the low current phase tends to increase χ . The quality of confinement is determined by balance of these competing effects.) We have analyzed a TFTR L-mode current ramp experiment. Before ramping, the experiment had $I_P = 2$ MA, and $\tau_E = 103$ ms. After the ramp, $I_P = 1$ MA and τ_E was nearly unchanged, $\tau_E = 100$ ms. The prediction from ITER89-P is that τ_E should have decreased from 123 ms to 67 ms, nearly a factor of two.

The power balance code (using q profiles from TRANSP²⁷) finds that τ_E is almost unchanged, going from 100 ms to 103 ms. Furthermore, the experimental central ion temperatures are reproduced within 10% both before and after.

Equations (1-4) may also explain the enhanced *core* confinement of H-modes. Much work has been done on the effects of rotation shear near the edge, which causes an edge temperature pedestal. However, confinement is observed to improve across the discharge, not just near the edge. This is consistent with the power balance code results, which find that increased edge temperatures translate into higher central temperatures and global confinement. For a typical L-mode with $T = 300$ eV at $r/a = 0.8$, increasing the temperature to 1 keV (typical of an H-mode pedestal) increases the global τ_E by a factor of roughly 1.5-2.0, which is a typical τ_E increase for H-modes. Unfortunately, Eqs. (1-4) are only valid at present for circular geometry and cannot yet be used to compare quantitatively to most H-modes which are in elongated plasmas with X -points. Also, rotation shear may sometimes be important in the core. Work is proceeding to include these effects.

Finally, note that several experiments have observed that temperature perturbations propagate much more rapidly than expected from the global confinement time. This type of qualitative behavior is predicted by Eqs. (1-4), if the plasma steady state being perturbed started close to marginal stability. Quantitative time-dependent simulations of perturbation experiments will be presented in the near future.

V. CONCLUSIONS

In summary, first principles simulations with kinetic effects have obtained quantitative agreement on core confinement ($0.25 < r/a < 0.8$) in a large number of L-mode discharges in TFTR. This high level of agreement with such a large number of discharges allows us to identify toroidal ion-temperature-gradient driven turbulence as the dominant transport

mechanism. Furthermore, qualitative agreement has been found with advanced confinement regimes such as supershots and hot ion modes, high ℓ_i modes and H-modes. More quantitative comparisons with supershots and H-modes will be possible when additional effects are added to the theory, specifically gradients of Z_{eff} , velocity shear, non-circular flux surfaces and trapped electron modes.

Nonlinear gyrofluid simulations find much stronger transport for the toroidal ITG mode than for the slab η_i mode; the toroidal instability is strong enough to force the temperature profile toward marginality in the inner half of the plasma. As a direct result, we find that the calculated temperature profiles are more sensitive to the linearly calculated threshold than to the nonlinearly calculated dependences of χ . However, we also showed that the plasma is typically not close to marginality at all radii, and that such an assumption, which is tantamount to ignoring the nonlinear simulation results, leads to egregious errors in the predicted profiles.

The theory finds that edge temperatures significantly influence core confinement. Thus, a quantitative understanding of edge confinement (not presented here) is required for a fully predictive calculation.

Finally, these first principles models are more accurate than empirical scaling laws such as ITER89-P and the RLW model, both in their quantitative ability to predict L-modes and in their ability to qualitatively explain enhanced confinement modes such as supershots, high ℓ_i modes, and the improved *core* confinement of H-modes. We therefore anticipate that in the near future, present microinstability simulation methods, properly employed, will offer a sounder quantitative scientific basis for the design of future fusion experiments.

Acknowledgments: We would like to thank the TFTR team for data and for valuable discussions. S. D. Scott, M. C. Zarnstorff, D. Mikkelsen, and K. McGuire have been particularly helpful. We would also like to thank R. E. Waltz for valuable discussions and insight. This work supported in part by two US Department of Energy (DOE) Postdoc-

toral Fusion Fellowships administered by the Oak Ridge Institute for Science Education, by DOE Contract Nos. DE-FG05-80ET-53088 and DE-AC02-76CH03073, and by the Numerical Tokamak Project (supported by the High Performance Computing and Communications Program and DOE). Computations were performed at the National Energy Research Supercomputer Center.³⁰

References

- ¹ M. Kotschenreuther, H. L. Berk, R. Denton, S. Hamaguchi, W. Horton, C.-B. Kim, M. LeBrun, P. Lyster, S. Mahajan, W. H. Miner, P. J. Morrison, D. Ross, T. Tajima, J. B. Taylor, P. M. Valanju, H. V. Wong, S. Y. Xiao, and Y.-Z. Zhang, in *Plasma Physics and Controlled Nuclear Fusion Research, 1990* (International Atomic Energy Agency, Vienna, 1991), Vol. 2, p. 361.
- ² A. M. Dimits and W. W. Lee, *J. Comput. Phys.* **107**, 309 (1993).
- ³ G. W. Hammett and F. W. Perkins, *Phys. Rev. Lett.* **64**, 3019 (1990).
- ⁴ G. W. Hammett, W. Dorland, and F. W. Perkins, *Phys. Fluids B* **4**, 2052 (1992).
- ⁵ W. Dorland, G. W. Hammett, L. Chen, W. Park, S. C. Cowley, S. Hamaguchi, and W. Horton, *Bull. Am. Phys. Soc.* **35**, 2005 (1990).
- ⁶ M. Kotschenreuther, *Bull. Am. Phys. Soc.* **36**, 2435 (1991).
- ⁷ R. E. Waltz, R. R. Dominguez, and G. W. Hammett, *Phys. Fluids B* **4**, 3138 (1992).
- ⁸ M. A. Beer, G. W. Hammett, W. Dorland, and S. C. Cowley, *Bull. Am. Phys. Soc.* **37**, 1478 (1992).
- ⁹ Several authors presented toroidal generalizations of the δf algorithm; *e.g.*, see Ref. 6. Toroidal generalizations of the gyrofluid equations appeared in Refs. 7 and 8.
- ¹⁰ R. J. Hawryluk, D. Mueller, J. Hosea, C. W. Barnes, M. A. Beer, M. G. Bell, R. Bell, H. Biglari, M. Bitter, R. Boivin, N. L. Bretz, R. V. Budny, C. E. Bush, L. Chen, C. Cheng, S. Cowley, D. Darrow, P. C. Efthimion, R. J. Fonck, E. Frederickson, H. P. Furth, G. Greene, B. Grek, L. R. Grisham, G. W. Hammett, W. W. Heidbrink, K. W. Hill, D. Hoffman, R. Hulse, H. Hsuan, A.

Janos, D. L. Jassby, F. C. Jobes, D. W. Johnson, L. C. Johnson, R. Kamperschroer, J. Kesner, C. Phillips, S. J. Kilpatrick, H. Kugel, P. H. LaMarche, B. LeBlanc, D. M. Manos, D. K. Mansfield, E. Marmor, E. Mazzucato, M. P. McCarthy, J. Machuzak, M. Mauel, D. C. McCune, K. McGuire, S. S. Medley, D. R. Mikkelsen, D. Monticello, Y. Nagayama, G. Navratil, R. Nazikian, D. K. Owens, H. Park, W. Park, S. F. Paul, F. W. Perkins, S. Pitcher, D. Rasmussen, M. H. Redi, G. Rewoldt, D. Roberts, A. L. Roquemore, S. Sabbagh, G. Schilling, J. Schivell, G. L. Schmidt, S. D. Scott, J. Snipes, J. Stevens, W. Stodiek, B. C. Stratton, J. Strachan, E. Synakowski, W. M. Tang, G. Taylor, J. Terry, J. R. Timberlake, H. H. Towner, M. Ulrickson, S. von Goeler, R. Wieland, J. Wilson, K. L. Wong, P. Woskov, M. Yamada, K. M. Young, M. C. Zarnstorff, and S. J. Zweben, *Fusion Technol.* **21**, 1324 (1992).

¹¹ W. Dorland, M. Kotschenreuther, M. A. Beer, G. W. Hammett, R. E. Waltz, R. R. Dominguez, P. M. Valanju, J. W. H. Miner, J. Q. Dong, W. Horton, F. L. Waelbroeck, T. Tajima, and M. J. LeBrun, "Comparisons of Nonlinear Toroidal Turbulence Simulations with Experiment", in *Plasma Physics and Controlled Nuclear Fusion Research 1994*, (to be published by the International Atomic Energy Agency, Vienna, 1995).

¹² M. A. Beer, Ph.D. thesis, Princeton University, 1995.

¹³ M. A. Beer, S. C. Cowley, and G. W. Hammett, "Field-Aligned Coordinates for Nonlinear Simulations of Tokamak Turbulence", Submitted to *Phys. of Plasmas* (unpublished).

¹⁴ M. Kotschenreuther, H. L. Berk, M. LeBrun, J. Q. Dong, W. Horton, J.-Y. Kim, Y. Kishimoto, D. W. Ross, T. Tajima, P. M. Valanju, H. V. Wong, W. Miner, D. C. Barnes, J. U. Brackbill, K. M. Ling, R. A. Nebel, W. D. Nystrom, J. A. Byers, T. J. Cohen, G. D. Kerbel, J. M. Dawson, R. D. Sydora, B. A. Carreras, N. Dominguez, C. L. Hedrick, J.-N. Leboeuf, H. Naitou, and T. Kamimura, in *Plasma Physics and Controlled Nuclear Fusion Research 1992* (International Atomic Energy Agency, Vienna, 1993), Vol. 2, p. 11.

- ¹⁵ G. W. Hammett, M. A. Beer, J. C. Cummings, W. Dorland, W. W. Lee, H. E. Mynick, S. E. Parker, R. A. Santoro, M. Artun, H. P. Furth, T. S. Hahm, G. Rewoldt, and W. M. Tang, "Advances in Simulating Tokamak Turbulent Transport," in *Plasma Physics and Controlled Thermonuclear Fusion Research 1994*, (to be published by the International Atomic Energy Agency, Vienna, 1995).
- ¹⁶ W. Dorland and G. W. Hammett, *Phys. Fluids B* **5**, 812 (1993).
- ¹⁷ R. E. Waltz, G. D. Kerbel, and J. Milovich, *Phys. of Plasmas* **1**, 2229 (1994).
- ¹⁸ W. Dorland, Ph.D. thesis, Princeton University, 1993.
- ¹⁹ M. Kotschenreuther, G. Rewoldt, and W. M. Tang, "Comparison of Initial Value and Eigenvalue Codes for Kinetic Toroidal Plasma Instabilities," Submitted to *Computer Physics Communications* (unpublished).
- ²⁰ R. Peccagnella, F. Romanelli, and S. Briguglio, *Nucl. Fusion* **30**, 545 (1990).
- ²¹ F. W. Perkins, C. W. Barnes, D. W. Johnson, S. D. Scott, M. C. Zarnstorff, M. G. Bell, R. E. Bell, C. E. Bush, B. Grek, K. W. Hill, D. K. Mansfield, H. Park, A. T. Ramsey, J. Schivell, B. C. Stratton, and E. Synakowski, *Phys. Fluids B* **5**, 477 (1993).
- ²² J. Q. Dong, W. Horton, and J. Y. Kim, *Phys. Fluids B* **4**, 1867 (1992).
- ²³ F. Romanelli and S. Briguglio, *Phys. Fl. B* **754** (1990).
- ²⁴ G. Bateman, *Phys. Fluids B* **4**, 634 (1992).
- ²⁵ D. R. Mikkelsen, S. D. Scott, H. G. Adler, M. A. Beer, M. G. Bell, C. E. Bush, W. Dorland, B. Grek, G. W. Hammett, K. W. Hill, D. W. Johnson, M. Kotschenreuther, D. K. Mansfield, H. K. Park, J. Schivell, E. J. Synakowski, and G. Taylor, *Bull. Am. Phys. Soc.* **39**, 1681 (1994).
- ²⁶ H. H. Towner, R. J. Goldston, G. W. Hammett, J. A. Murphy, C. K. Phillips, S. D. Scott, and

M. C. Zarnstorff, *Rev. Sci. Instrum.* **63**, 4753 (1992), (Proceedings of the 9th Topical Conference on High Temperature Plasma Diagnostics, Santa Fe).

²⁷ R. J. Hawryluk, in *Physics of Plasmas Close to Thermonuclear Conditions*, edited by B. Coppi, G. G. Leotta, D. Pfirsch, R. Pozzoli, and E. Sindoni (Pergamon Press, New York, 1980), Vol. 1, Chap. 2, p. 19.

²⁸ P. N. Yushmanov, T. Takizuka, K. S. Riedel, O. J. W. F. Kardaun, J. G. Cordey, S. M. Kaye, and D. E. Post, *Nuclear Fusion* **30**, 1999 (1990).

²⁹ S. D. Scott, private communication (unpublished).

³⁰ *World Survey of Activities in Controlled Fusion Research*, edited by C. Bobeldijk (International Atomic Energy Agency, Vienna, 1991), p. 159.

Figure Captions

1. TFTR NTP Test Case. The predicted ion temperature (shown in the top panel) lies within the error bars. The predicted χ_i increases strongly with minor radius despite the decreasing temperature.
2. TFTR NTP Test Case. The departure from criticality ($L_{Tcrit}/L_T > 1$) is significant and increases toward the edge for the profile predicted by the full theory (solid line). [For $r/a < 0.1$, neoclassical transport relaxes the gradient below the critical gradient.] The dotted line represents the profile whose gradient is everywhere critical – it is clearly wrong compared to the experimental data (the dashed line), thus demonstrating the importance of the nonlinear simulations.
3. Comparison of predicted energy confinement times for the IFS-PPPL transport model, the RLW model, and ITER89-P for 60 TFTR discharges.
4. The theory correctly predicts the temperature profiles as the power is varied by a factor of four.
5. The theory correctly predicts the temperature variation as the current is changed by nearly a factor of two.
6. The ratio of the predicted $T_i(r)$ to the measured $T_i(r)$ for 70 TFTR L-mode discharges (shown in yellow), with widely varying current, power, density, *etc.*; the average and the standard deviation of these curves are shown in black. The blue and green curves represent the average and standard deviation of predictions obtained as C_0 is artificially varied by a factor of two up and down respectively.

7. The theory qualitatively reproduces the enormous change in ion temperature observed between L-modes and supershots. Most of the improvement in confinement comes from the strong dependence of $R/L_{T_{\text{crit}}}^{(1)}$ on high T_i/T_e and from the high edge temperature. The temperature is also sensitive to the hollowness of the $Z_{\text{eff}}(r)$ profile. The solid curve is predicted by the theory if Z_{eff} rises parabolically from 2 to 5; the dashed curve is predicted if Z_{eff} rises from 2.5 to 4.

Table I. TFTR Power Scan, comparing the energy confinement times from experimental measurement, the theoretical prediction, and the ITER89-P empirical fit.

<i>Shot#</i>	P_h (MW)	τ_{Exp} (ms)	τ_{Theory}	τ_{ITER89P}
64975	18.7	94	91	72
65025	9.0	147	145	99
64986	4.6	172	159	140

Table II. TFTR Current Scan, comparing the energy confinement times from experimental measurement, the theoretical prediction, and the ITER89-P empirical fit.

<i>Shot#</i>	I_p (MA)	τ_{Exp} (ms)	τ_{Theory}	τ_{ITER89P}
45603	1.2	75	79	81
41328	1.8	103	103	106
45600	2.1	130	140	128

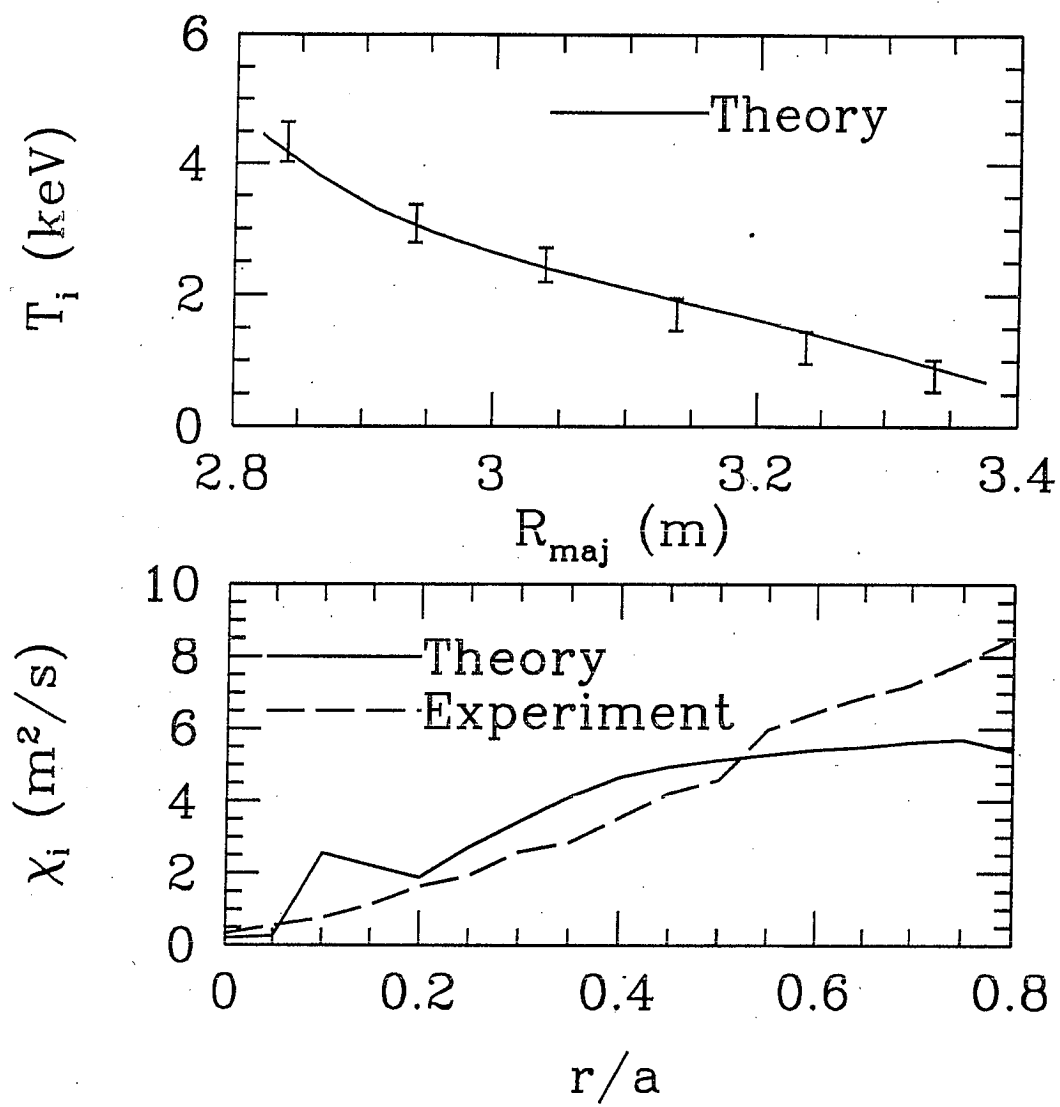


FIG. 1.

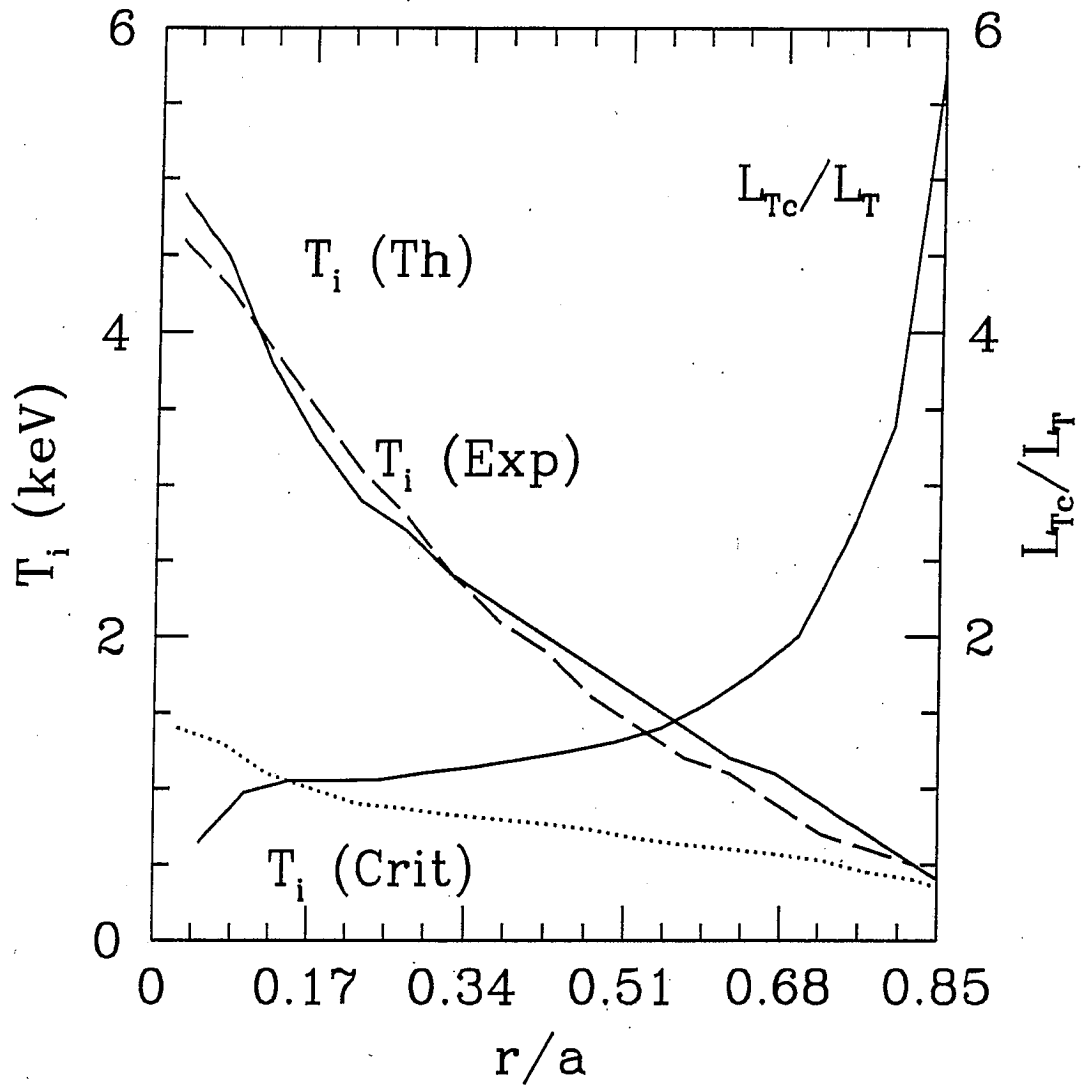


FIG. 2.

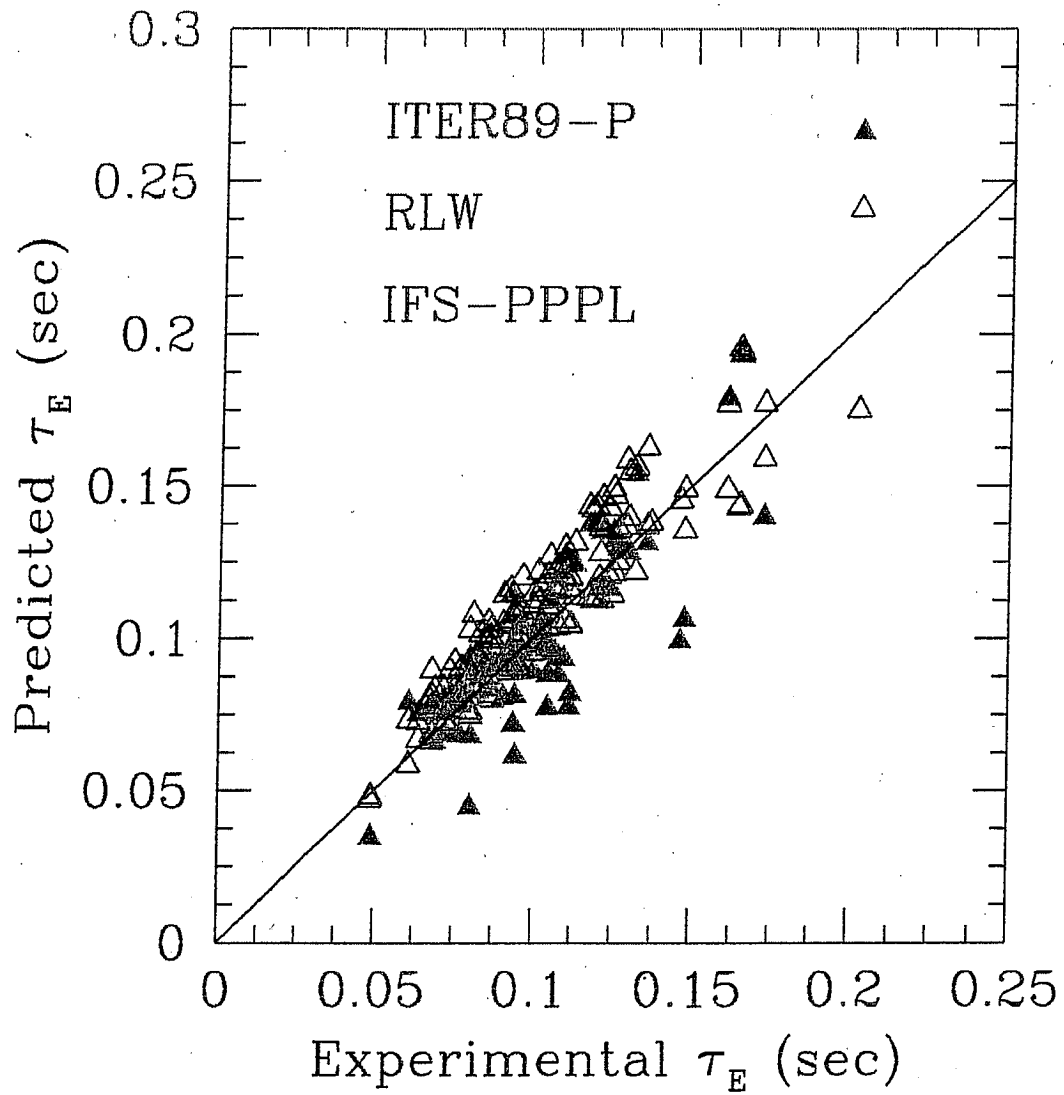


FIG. 3.

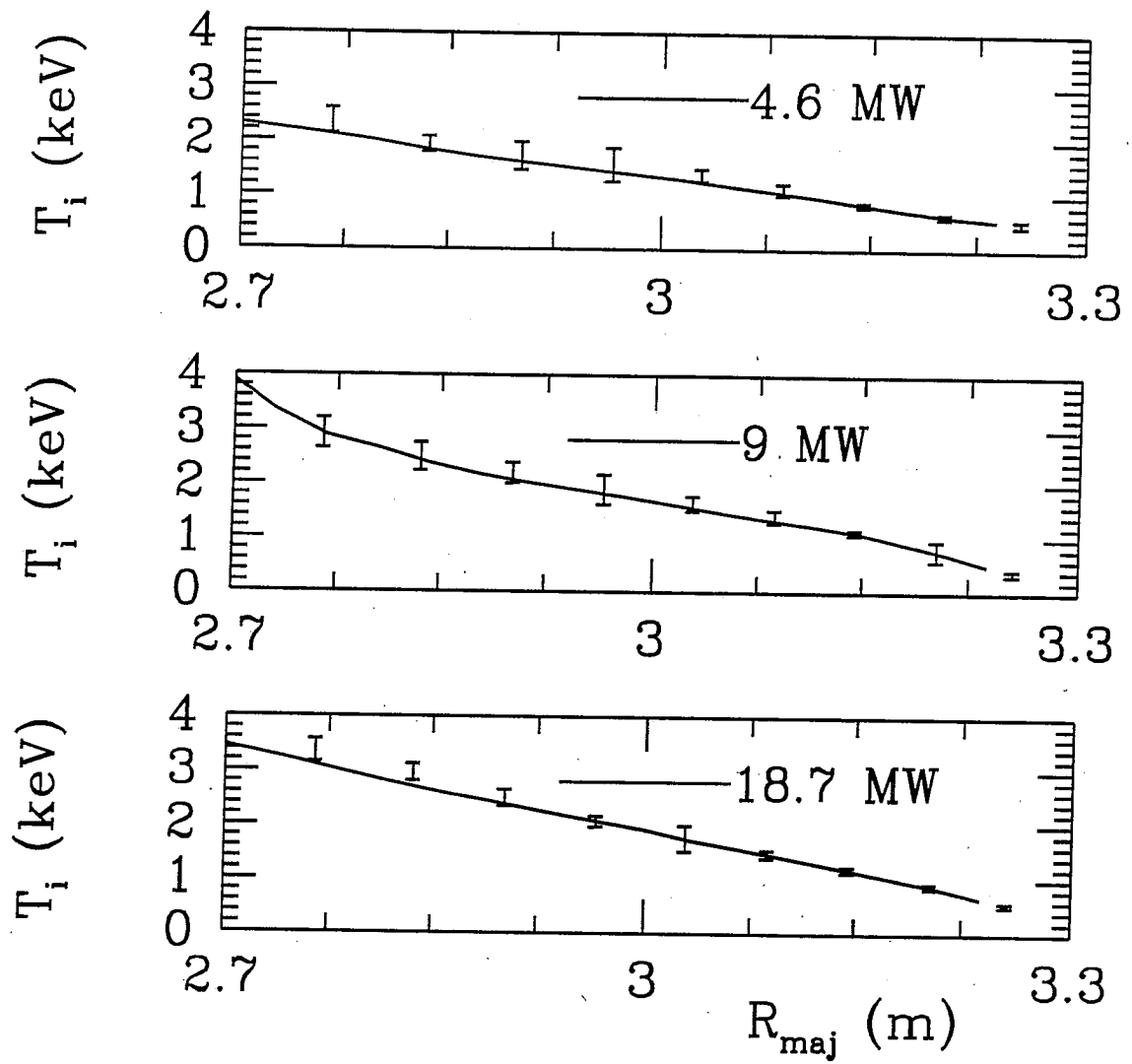


FIG. 4.

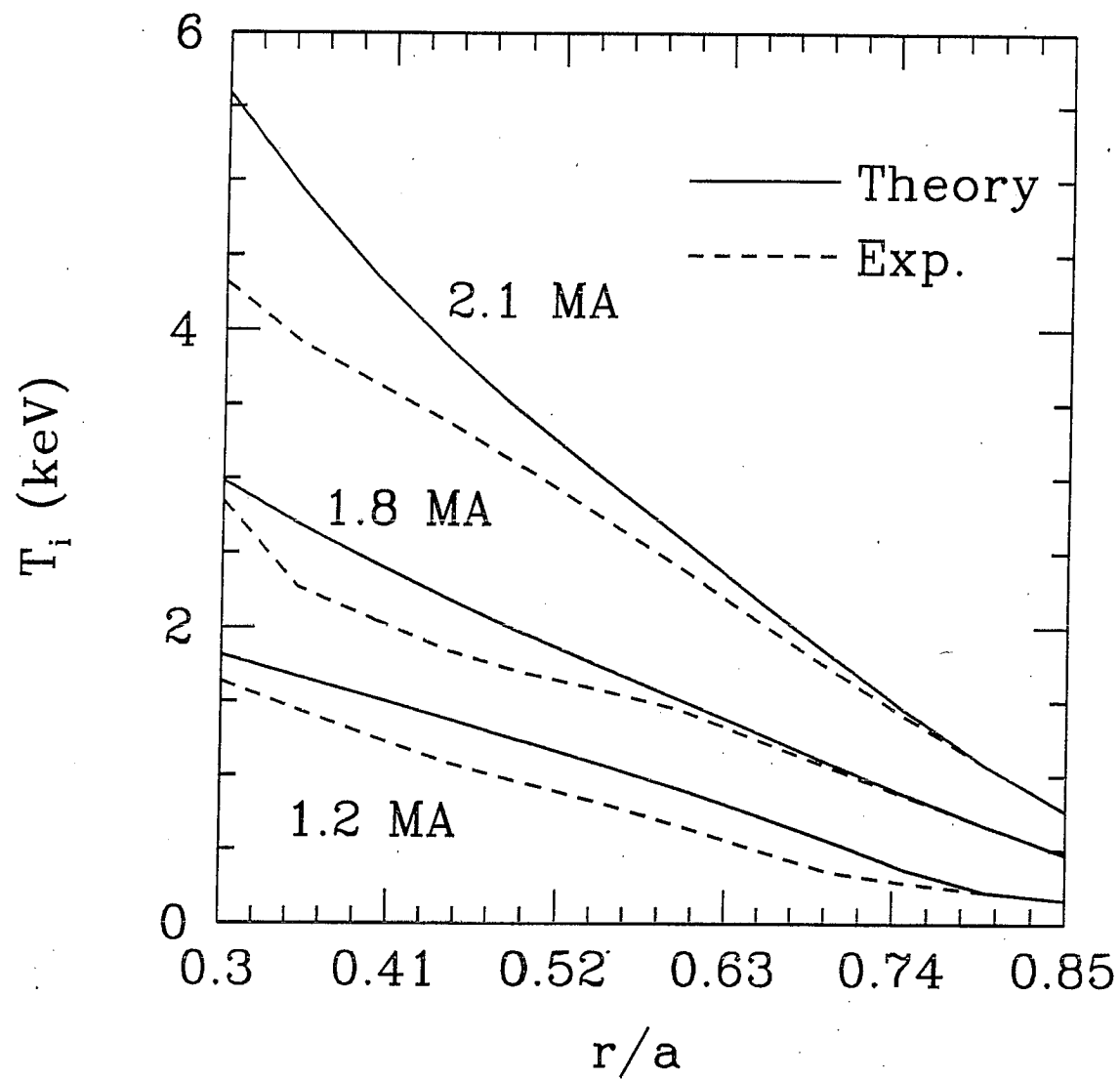


FIG. 5.

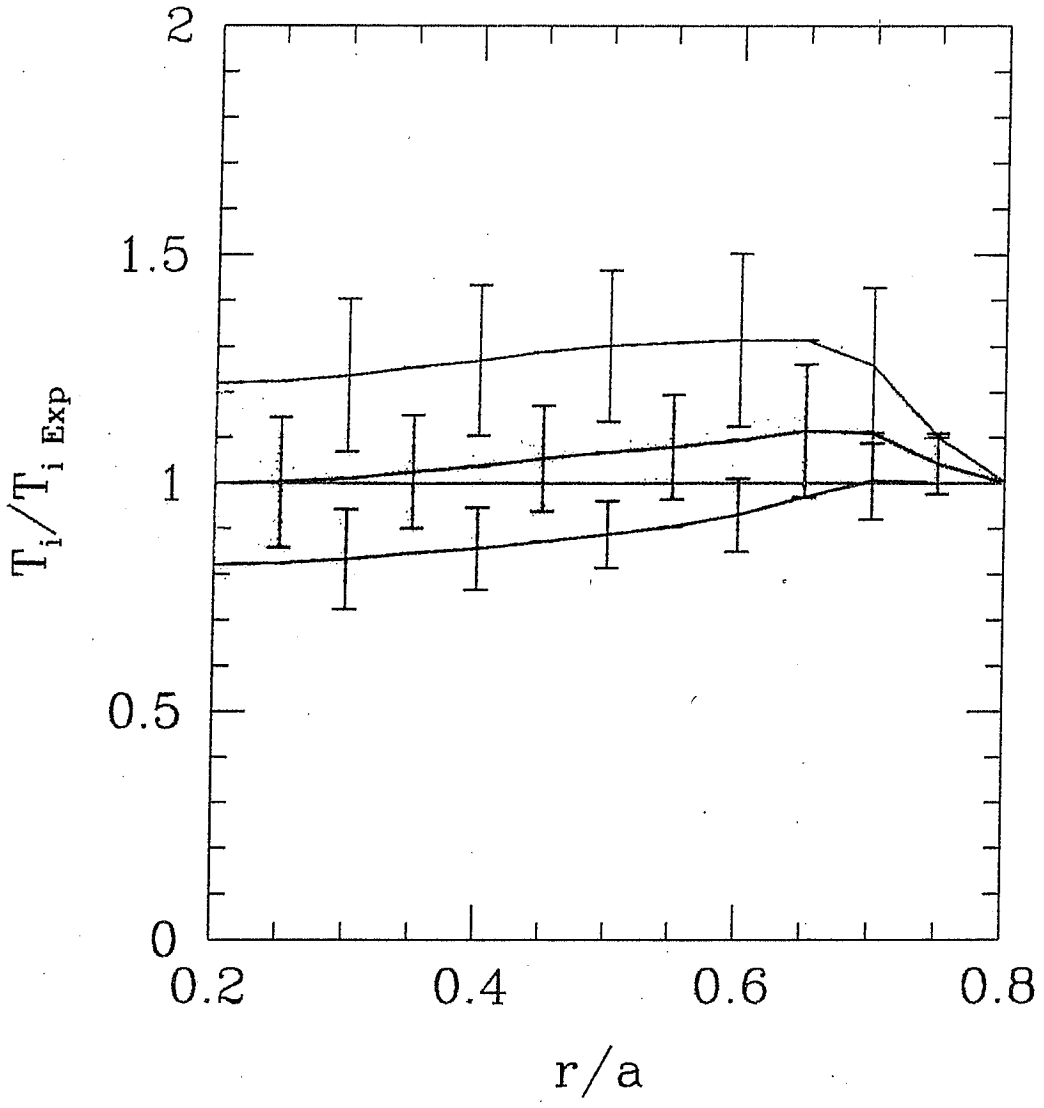


FIG. 6.

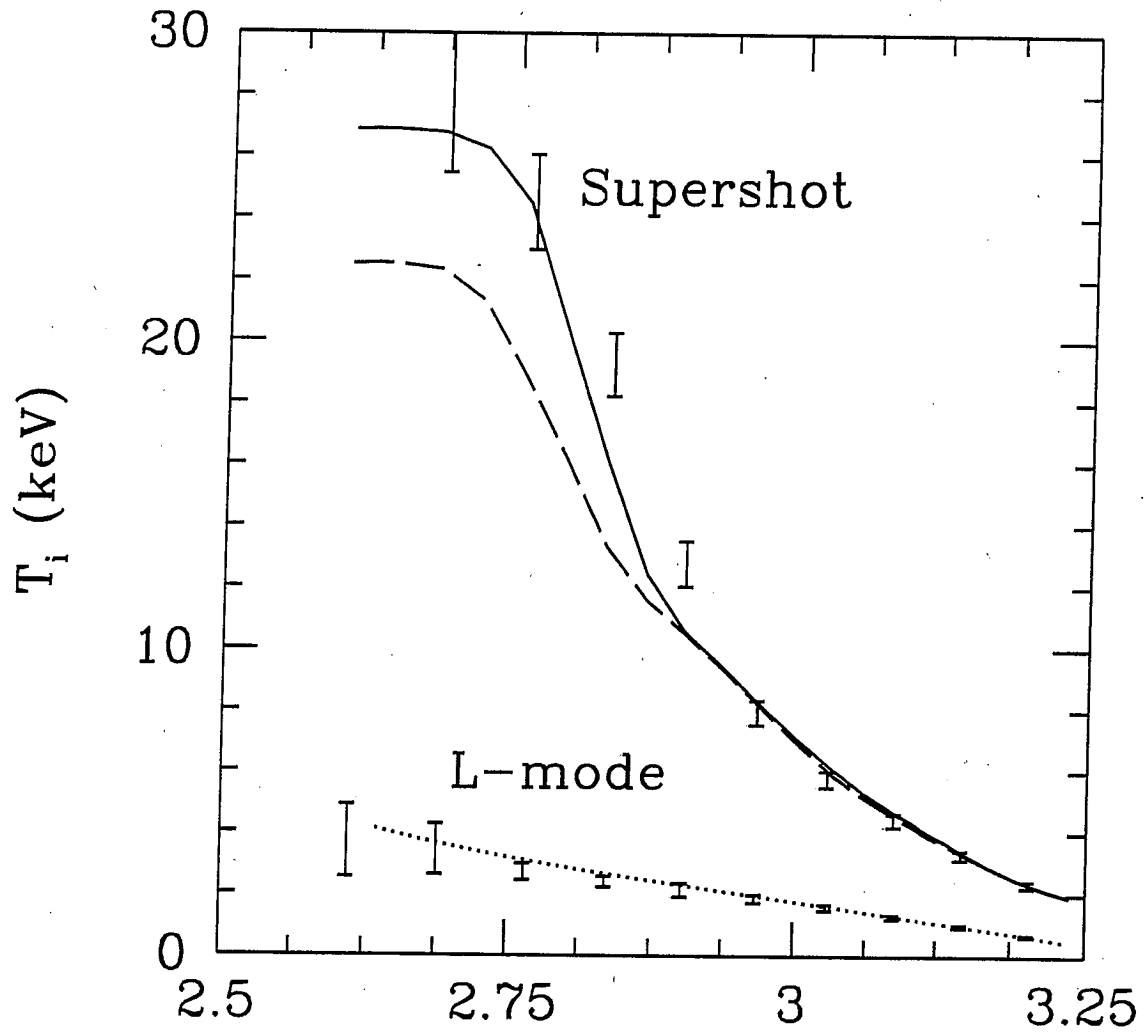


FIG. 7.